Article

Dual-Level Enhanced Nonradiative Carrier Recombination in Wide-Gap Semiconductors: The Case of Oxygen Vacancy in SiO$_2$

Chen Qiu, Yu Song,* Hui-Xiong Deng,* and Su-Huai Wei*

Read Online

ACCESS | Metrics & More | Article Recommendations

ABSTRACT: The conventional single-defect-mediated Shockley−Read−Hall model suggests that the nonradiative carrier recombination rate in wide-band gap (WBG) semiconductors would be negligible because the single-defect level is expected to be either far from valence-band-maximum (VBM) or conduction-band-minimum (CBM), or both. However, this model falls short of elucidating the substantial nonradiative recombination phenomena often observed experimentally across various WBG semiconductors. Owing to more localized nature of defect states inherent to WBG semiconductors, when the defect charge state changes, there is a pronounced structural relaxation around the local defect site. This suggests that a defect at each charge state may exhibit a few distinct local configurations, namely, a stable configuration and a few metastable/transit state configurations. Consequently, a dual-level nonradiative recombination model should more realistically exist in WBG semiconductors. In this model, through the dual-level mechanism, electron and hole trap levels are different from each other and could be closer to the CBM for the electron trap and closer to the VBM for the hole trap, respectively; therefore, this significantly increases the corresponding electron and hole capture rates, enhancing the overall process of nonradiative recombination, and explains the experimental observations. In this work, taking technically important SiO$_2$ as an illustrative example, we introduce the dual-level mechanism to elucidate the mechanism of nonradiative carrier recombination in WBG semiconductors. Our findings demonstrated strong alignment with available experimental data, reinforcing the robustness of our proposed dual-level model. Our fundamental understanding, therefore, provides a clear physical picture of the issue and can also be applied to predict the defect-related nonradiative carrier recombination characteristics in other WBG materials.
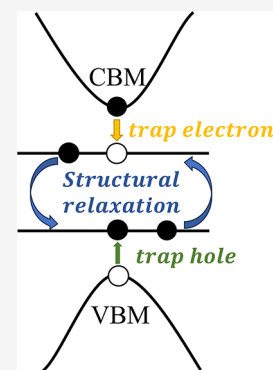
INTRODUCTION

Defect-mediated nonradiative recombination, i.e., Shockley−Read−Hall (SRH) recombination,[1,2] plays an important role in determining the performance and reliability of semiconductor devices.[3,4] In relatively narrow bandgap semiconductors, e.g., Si and GaAs, the recombination process has conventionally been characterized by a single-defect transition level, where holes and electrons are trapped and recombined.[5−8] In general, holes tend to be more readily captured by a defect level positioned near the valence band maximum (VBM), whereas capturing electrons from the conduction band minimum (CBM) by the same defect level can be challenging. Conversely, a defect level situated close to the CBM can effectively capture electrons but faces difficulties in capturing holes. Consequently, the nonradiative recombination process is constrained by the lower capture rate between hole and electron traps. For this reason, the prevailing consensus is that only defect levels positioned near the middle of the bandgap can function as effective nonradiative recombination centers, as they enable the simultaneous capture of both electrons and holes with relative ease.[5] However, for wide-band gap (WBG) materials, such as SiO$_2$, HfO$_2$, and GaN, when the defect level is positioned near the middle of the bandgap, it is considerably distant from the VBM and CBM. According to the

conventional single-level SRH model for WBG materials, the rate of nonradiative carrier recombination in these materials should be small. Nevertheless, this is clearly inconsistent with the experimental observations, as many oxides and nitrides exhibit a significant carrier-mediated nonradiative recombination rate.[9−16] Therefore, the conventional single-level SRH model faces a conundrum when it comes to comprehending the substantial nonradiative recombination rates observed in WBG materials. It is imperative to elucidate new nonradiative recombination mechanisms in these materials.

Taking SiO$_2$, which is widely utilized in metal-oxide-silicon (MOS) systems, is an illustrative example. When these devices work under specific environments like outer space, nuclear reactors, etc., the ionizing radiation could produce a significant amount of defects during operation. These defects have the potential to induce nonradiative recombination of the carriers,
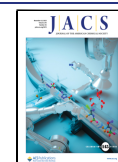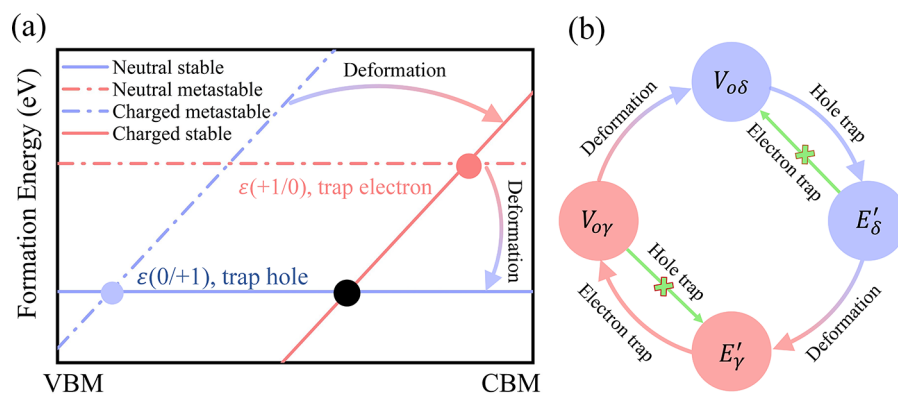
Figure 1. (a) Schematic plot of dual-metastable defect configurations enhanced nonradiative carrier recombination. (b) Nonradiative recombination processes of oxygen vacancy in amorphous SiO$_2$.

leading to the degradation of microelectronic device performance. Extensive research conducted over the past decades has revealed that the pronounced nonradiative recombination of electron−hole pairs induced by ionizing irradiation is primarily attributed to two distinct oxygen vacancy defects in SiO$_2$. They exhibit two distinct local structures, one characterized by a dimer configuration (denoted as $V_{o\delta}$ in its neutral state and as E'_{δ} in its positively charged state) and the other featuring a 4-fold puckered structure (denoted as $V_{o\gamma}$ in its neutral state and as E'_{γ} in its positively charged state).[17−21] Experimentally, it is evident that during hole injection, both E'_{δ} and E'_{γ} defects are generated at high densities, which are usually attributed to the large hole nonradiative recombination capture-rate of $V_{o\delta}$ and $V_{o\gamma}$, while the rapid decrease of E'_{δ} and E'_{γ} concentrations after electron injection into the SiO$_2$ sample is also attributed to the large electron nonradiative recombination capture-rate of E'_{δ} and E'_{γ}. These phenomena highlight the significant nonradiative recombination effect of oxygen vacancy in SiO$_2$.[10,22] Previous research widely supports the notion that this nonradiative recombination primarily occurs through the single defect transition level, i.e., $V_{o\delta}$ and E'_{δ} (or $V_{o\gamma}$ and E'_{γ}) in SiO$_2$.[10,22] However, it is worth noting that the defect levels of E'_{δ} and $V_{o\gamma}$ are quite deep, nearly in the middle of the SiO$_2$ band gap (~4.5 eV above VBM).[19] Based on the analysis of the single-level SRH model, it seems unlikely that a single-level, such as $V_{o\delta}$ and E'_{δ} (or $V_{o\gamma}$ and E'_{γ}) alone, could account for the observed strong nonradiative recombination in SiO$_2$. Therefore, the mechanism behind the experimentally observed strong nonradiative recombination in WBG materials like oxide SiO$_2$ remains elusive and warrants further investigation for a more comprehensive understanding.

In this work, we introduce a general dual-level nonradiative recombination picture and provide fundamental insights into the enhancement of the nonradiative carrier recombination by coupling two metastable defect configurations together in WBG oxides. Specifically, these metastable defect configurations bring the electron and hole trap levels into closer proximity to the CBM and VBM, respectively. This proximity significantly increases the corresponding electron and hole capture rates, consequently enhancing the whole process of the nonradiative recombination (see Figure 1 a). More specifically, initially, the hole trap level of the neutral defect state ($V_{o\delta}$) is closer to the VBM, facilitating the trapping of a hole to form a metastable charged defect center (E'_{δ}). Subsequently, this metastable charged structure (E'_{δ}) rapidly undergoes deformation to establish a stable charged configuration (E'_{γ}) after

overcoming a minor barrier. Following this, the stable charged state (E'_{γ}) efficiently captures an electron to generate metastable neutral defect center ($V_{o\gamma}$), given its proximity to the CBM. Lastly, the metastable neutral defect center ($V_{o\gamma}$) surpasses a small energy barrier and promptly transforms into the stable neutral state ($V_{o\delta}$), thus completing the entire cycle of nonradiative hole−electrons recombination, as shown in Figure 1b. The fundamental understanding of the dual-level mechanism proposed here provides a general and significant way to investigate nonradiative recombination in other WBG materials.

■ METHOD

Our first-principles calculations of electronic structure and total energy are carried out using spin-polarized density-functional theory (DFT), as implemented in the PWmat package, with the NCPP-SG15-PBE pseudopotentials[23−26] for the exchange-correlation functional. To improve the accuracy of the total energy and electronic band structure, the Heyd−Scuseria−Ernzerhof (HSE06) hybrid functional method[27] with a mixing parameter of 50% is employed. A 216-atom supercell is employed to study the properties of oxygen vacancies in amorphous SiO$_2$ (a-SiO$_2$). The calculated lattice constant of a-SiO$_2$ is $a = b = 16.49$ and $c = 12.09$ Å with a bandgap $E_g = 9$ eV, in good agreement with experiment.[28] All atoms within the supercell are relaxed until the forces on each atom fall below 0.01 eV/Å and the plane-wave energy cutoff for the basis-functions is set to 60 Ry. The formation energy (ΔH_f) of a defect α at charge state q is determined according to ref 29 as follows:

$$\Delta H_f(\alpha, q) = \Delta E(\alpha, q) + \sum_i n_i \mu_i + q E_F \tag{1}$$

where $\Delta E(\alpha, q) = E(\alpha, q) - E(\text{host}) + \sum_i n_i E_i + q E_{VBM}^{host}$. μ_i is the chemical potential of each of the components i and E_i represent the energy of the elemental stable solid/gas; n_i denotes the number of atoms removed from the host supercell to form supercell containing the defect α. q describes the number of electrons transferred from the supercell to the reservoirs. The defect transition level $\varepsilon_\alpha(q/q')$ is defined as the Fermi level (E_F), at which the formation energy for defect with charge state q and q' are equal, that is

$$\varepsilon_\alpha(q/q') = [\Delta E(\alpha, q) - \Delta E(\alpha/q')]/(q' - q) \tag{2}$$

According to static coupling approximation,[30,31] the electron−phonon coupling constant can be obtained within one self-consistent field calculation.[23,32,33] Then, the non-radiative decay probability (W_{ij}) can be calculated by the first-principles method:[34]

$$W_{ij} = \left(\frac{\pi kT}{\lambda}\right)^{1/2} \left(\sum_k \frac{1}{\omega_k^2} |C_{i,j}^k|^2\right) \exp\left[-\frac{(E_i - E_j - \lambda)^2}{4kT\lambda}\right]$$

(3)

where $C_{i,j}^k$ is the electron−phonon coupling constant between electronic states i and j, as well as phonon mode k. λ is the reorganization energy (structural relaxation energy between initial and final configurations after the charge state transition from i to j). T is the temperature, and ω_k is the frequency of the kth harmonic phonon mode. The carrier-capture-rate coefficient can be calculated by $B = W_{ij}V$ after obtaining the nonradiative decay probability W_{ij}, where V is the supercell volume. The capture cross-section σ is defined by $\sigma = B/\sqrt{3k_BT/m^*}$, where k_B is the Boltzmann constant and m^* is the effective mass of the carrier. The effective mass of the electron and hole of SiO_2 is 0.3 m_e and 0.58 m_e, respectively.[35,36] The m_e is the mass of electrons.

RESULTS AND DISCUSSION

As shown in Figure 2, the oxygen vacancy in SiO_2 can take two distinct defect configurations: a dimer structure (with neutral state $V_{o\delta}$ and positively charged state E_δ') and a 4-fold puckered structure (with neutral state $V_{o\gamma}$ and positively charged state E_γ'). In the neutral $V_{o\delta}$ shown in Figure 2a, an oxygen atom is removed, and the two nearest Si atoms bond together in a dimer configuration with a Si−Si bond length of 2.56 Å. When
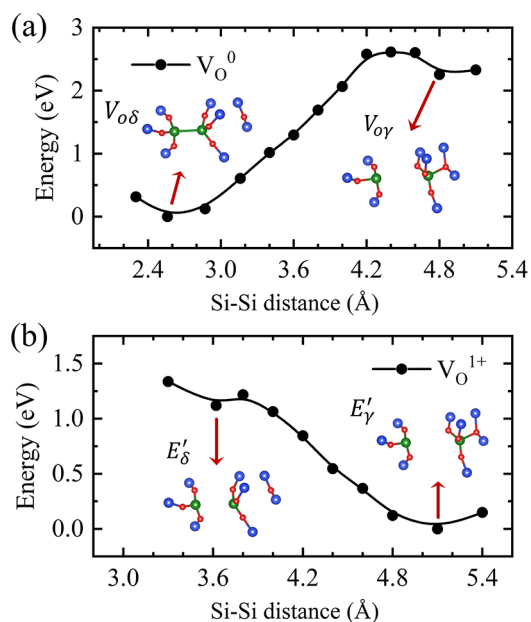

Figure 2. Relative energies of the (a) neutral and (b) positively charged oxygen vacancy as a function of the Si−Si distance in SiO_2. The inset shows the atomic configuration, e.g., neutral dimer structure $V_{o\delta}$, positively charged dimer structure E_δ', neutral puckered configuration $V_{o\gamma}$, and positively charged puckered configuration E_γ'. Blue and red balls are Si atoms and O atoms, respectively. The Si atoms next to the oxygen vacancy are highlighted as green balls.

this defect center is positively charged to form the E_δ' structure of oxygen vacancy, the removal of a bonding electron leads to an elongated weak Si−Si bond of 3.61 Å. This structure, however, is only metastable. The positively charged Si+ can move further toward the next nearest neighbor oxygen ion to form the stable 4-fold puckered configuration E_γ', resulting in a longer Si−Si bond length of 5.09 Å. Indeed, it is easy to move from the metastable E_δ' to E_γ' configuration, as the energy barrier is only 0.11 eV.[28,37] As shown in Figure 2a,b, the local structure of metastable $V_{o\gamma}$ is similar to that of E_γ'. However, the formation energy of $V_{o\gamma}$ is more than 2 eV higher than that of $V_{o\delta}$, and $V_{o\gamma}$ can relax to the $V_{o\delta}$ structure by overcoming a 0.35 eV barrier.[28,37]

In order to gain a deeper understanding of the nonradiative recombination process of oxygen vacancies in SiO_2, as depicted in Figure 3, we carefully examined the defect transition levels
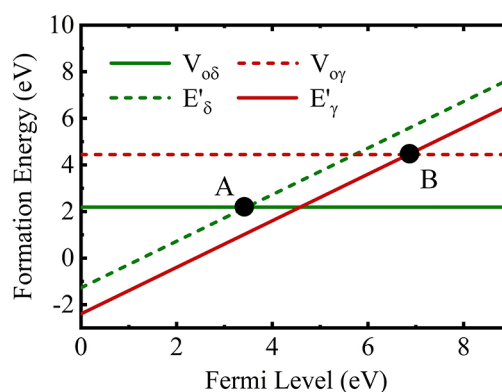

Figure 3. HSE06-calculated formation energies of dimer configuration at neutral ($V_{o\delta}$) and positively charge (E_δ') states as well as 4-fold puckered structure at neutral ($V_{o\gamma}$) and positive charge (E_γ') states in SiO_2 as functions of Fermi level.

of both types of oxygen vacancies. Figure 3 illustrates the formation energies of both the dimer and puckered structures of oxygen vacancies in neutral and positively charged states as functions of E_F. The E_F value ranges from the valence band maximum (VBM) to conduction band minimum (CBM), that is, from 0 to 9 eV for SiO_2.[28] According to the SRH model, for $V_{o\delta}$ and E_δ', the first step of the nonradiative recombination process involves the trapping of a hole by $V_{o\delta}$, which occurs through (0/+1) transition level at point A with a value of 3.5 eV above the VBM. The calculated hole capture cross-section of $V_{o\delta}$, is $\sigma_p \cong 1.6 \times 10^{-11}$ cm^2 (see Table 1), in good agreement with the previous experimental report.[10] After a hole is captured, the $V_{o\delta}$ fully relaxes to a metastable E_δ' configuration. The second step involves the trapping of an electron from the CBM by fully relaxed E_δ', which also occurs at the (+1/0) transition level at point A for the single-level SRH model. This transition level is exceptionally deep, approximately 5.5 eV below the CBM, resulting in a minuscule electron capture cross-section ($\sigma_n < 10^{-20}$ cm^2) for E_δ'. In other words, it is almost impossible for E_δ' to capture electrons from the CBM and become $V_{o\delta}$, that is, $V_{o\delta}$ is a hole trap state, not a nonradiative recombination center, as indicated in Figure 1.

A similar issue has also arisen in the nonradiative recombination process only involving $V_{o\gamma}$ and E_γ'. In Figure 3, the defect transition level for (0/+1) (point B) is shown to be 6.8 eV above the VBM, while the transition level for (+1/0) is 2.2 eV below the CBM. This suggests that the dominant

Table 1. Calculated Electron Capture Cross-Section, σ_n (cm²), and Hole Capture Cross-Section, σ_p (cm²), through Transition Levels at Points A and B in Figure 3[a]

	electron trapping				hole trapping			
	σ_n	B_n	λ	W_{ij}	σ_p	B_p	λ	W_{ij}
A	$<10^{-20}$	5.3×10^{-20}	2.37	16	1.6×10^{-11}	2.4×10^{-4}	2.52	7.3×10^{16}
B	3.2×10^{-14}	6.9×10^{-7}	1.14	2.1×10^{14}	$<10^{-20}$	$<10^{-20}$	1.55	$<10^{-20}$

[a]Calculated electron-, hole-capture-rate coefficients, B_n and B_p (cm³ s⁻¹), nonradiative decay probabilities, W_{ij} (s⁻¹), and relaxation energy, λ (eV) are listed in this table.
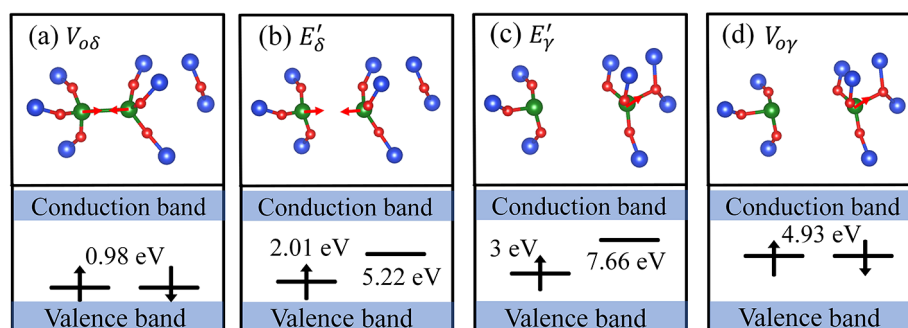

Figure 4. Ball-and-stick schematic plot of local atomic relaxation around the oxygen vacancy in (a) $V_{o\delta}$, (b) E'_{δ}, (c) E'_{γ}, and (d) $V_{o\gamma}$. The calculated single-particle levels, with reference to the host VBM, are also plotted for each charge state. Blue and red balls are Si and O atoms, and the neighboring Si atoms of the oxygen vacancy are highlighted as green balls. The spin-up and spin-down channels are denoted by upward- and downward-pointing arrows, respectively. The red arrows imply the directions of the atomic movements near oxygen vacancy.

electron-trapping process of E'_{γ} may occur through the transition level at point B. This is because the $(+1/0)$ transition level at point B is relatively shallow, indicating a high electron capture cross-section of E'_{γ} ($\sigma_n \cong 3.2 \times 10^{-14}$ cm²), in accordance with the experimental result.[10] Hence, E'_{γ} can capture an electron and relax into $V_{o\gamma}$ configuration; however, the $(0/+1)$ transition level at point B is extremely deep, indicating a low hole capture cross-section ($\sigma_p \ll 10^{-20}$ cm²) of $V_{o\gamma}$ and hardly captures one hole and returns back to E'_{γ}, that is, E'_{γ} is an electron trap state instead of a nonradiative recombination center. One can see that if the nonradiative recombination processes of dimer structure ($V_{o\delta}$ and E'_{δ}) and 4-fold puckered configuration ($V_{o\gamma}$ and E'_{γ}) are isolated from each other, then a high density of E'_{γ} cannot be observed in SiO₂ sample after hole injection, and the rapid decrease of E'_{δ} after electron injection cannot be observed, neither.[10] Therefore, the conventional understanding of the nonradiative recombination process only involving the single oxygen-vacancy defect level has encountered a predicament.

Because the $V_{o\gamma}$ and E'_{δ} are metastable configurations, assuming an attempt frequency of 10^{13} s⁻¹,[38] we estimate that the time for the neutral state to transform from $V_{o\gamma}$ to $V_{o\delta}$ is in about 70 ns and for the positively charge state to transform from E'_{δ} to E'_{γ} is in approximately 1 ns based on ref 39, which is much faster than the time it takes for hole and electron trapping due to the exceedingly small carrier capture rate of $V_{o\gamma}$ and E'_{δ} (see Table 1). Therefore, $V_{o\gamma}$ can easily relax to $V_{o\delta}$ and E'_{δ} can transform to E'_{γ} after overcoming a small barrier. Thus, the nonradiative recombination processes of $V_{o\delta}$, E'_{δ} and $V_{o\gamma}$, E'_{γ} could be synergistic rather than isolated, as presented in Figure 1. Accordingly, we propose a new understanding of nonradiative recombination processes of oxygen vacancies in SiO₂ through a metastable-structure-relaxation mechanism, as exhibited in Figure 1. The first step of the nonradiative recombination process is for $V_{o\delta}$ to trap one hole from the VBM through a $(0/+1)$ transition level at point A and become

the metastable positively charged state E'_{δ} center, resulting in a hole-trapping process. Then, overcoming a small barrier allows the transition from the metastable E'_{δ} configuration to the E'_{γ} configuration. Next, electron trapping of E'_{γ} occurs through the $(+1/0)$ transition level at point B, followed by the E'_{γ} center fully relaxing to the metastable $V_{o\gamma}$ structure. Finally, a small barrier can be easily overcome to move from the metastable $V_{o\gamma}$ to the $V_{o\delta}$ configuration.

As discussed above, the high concentration of E'_{γ} observed after hole injection and the decrease in concentrations of E'_{δ} after electron injection in SiO₂ sample can be attributed to the deformation of metastable E'_{δ} and $V_{o\gamma}$ structures. Consequently, the dilemma surfaced from the conventional wisdom of nonradiative recombination of oxygen vacancy is well reconciled by the metastable-structure-relaxation mechanism. It is important to point out that the effective nonradiative recombination center of conventional single-level SRH recombination in ultrawide bandgap semiconductors has difficulty capturing both carriers from the band edge because the single defect level is always far from either the CBM or VBM, or both, and in general, defect levels far from the VBM are more difficult to capture holes, while those far from the CBM are more difficult at trapping electrons.[32,40] Therefore, the dual-metastable defect configuration enhanced nonradiative carrier recombination mechanism should be a fundamental way to understand the nonradiative recombination in ultrawide bandgap semiconductors.

To further unveil the physical origin of the nonradiative recombination of oxygen vacancies, we carefully examined the local atomic structures and single-particle levels for dimer and 4-fold puckered configurations, as shown in Figure 4. When an oxygen atom is removed from the host structure, two bonds are broken, forming two dangling bonds. For $V_{o\delta}$ system, the two Si atoms closest to the oxygen vacancy site form a dimer structure and the two dangling bond states form a fully occupied bonding and a fully empty antibonding state, thus

this atomic displacement-induced level coupling between the two dangling bonds can lead to an electronic energy gain,[41] resulting in a shallow defect level of 0.98 eV above VBM. Consequently, the hole capture cross-section of $V_{o\delta}$ is quite large, which allows it to readily capture a hole from the valence band and become an E_δ' center. However, we observed that for the E_δ' system, the two Si atoms closest to the oxygen vacancy move away from the vacancy site due to weakening of the dimer bond and Coulomb attraction from neighboring oxygen ions, leading to the shift of the defect level toward the center of the gap. However, the resulting unoccupied defect level in the E_δ' structure is still 3.78 eV below the CBM. Therefore, the electron capture cross-section of E_δ' is very small because the deep unoccupied defect level cannot trap an electron efficiently from the conduction band. Owing to the disparity in electronegativity between Si and O atom, Si atoms within SiO_2 inherently exhibit cationic traits, whereas O atoms demonstrate an anionic characteristic. Consequently, Coulomb attraction between the positively Si dangling bond state and neighboring oxygen ion can lead to the formation of the E_γ' center, which has a high energy level and large spin-splitting of the degenerate orbital. Because the unoccupied defect level is close to the CBM and located at 1.34 eV below the CBM, E_γ' possesses a large electron capture cross-section, so it can capture an electron and covert it to $V_{o\gamma}$. Finally, in the 4-fold puckered $V_{o\gamma}$ configuration, the breaking of the Si dimer bond shifts the defect level upward and is 4.93 eV above the VBM. Indeed, the hole capture cross-section for $V_{o\gamma}$ is minimal and almost impossible to trap one hole from the VBM.

CONCLUSIONS

In conclusion, we have demonstrated the concepts and principles of the dual-level nonradiative recombination mechanism by investigating the nonradiative recombination of oxygen vacancies in SiO_2, involving four distinct processes: (i) $V_{o\delta}$ captures a hole from the valence band, forming the metastable state E_δ', (ii) the metastable E_δ' relaxes to stable E_γ' after overcoming a small energy barrier, (iii) the E_γ' captures an electron from the conduction band to form the metastable state $V_{o\gamma}$, and (iv) a small energy barrier can be overcome to transfer from the metastable $V_{o\gamma}$ to the stable $V_{o\delta}$ configuration. The shallow defect level of $V_{o\delta}$ results in a significant hole capture cross-section of $V_{o\delta}$. Conversely, the unoccupied defect level of E_γ' close to the CBM leads to a substantial electron capture cross-section of E_γ'. Our findings not only provide a fundamental and comprehensive understanding of the origin of nonradiative recombination involving oxygen vacancies in SiO_2 but also explain the concepts and principles of the dual-level nonradiative recombination mechanism, which are expected to have broader applicability in understanding nonradiative recombination in other wide-band gap semiconductors.

AUTHOR INFORMATION

Corresponding Authors

Yu Song − *College of Physics and Electronic Information Engineering, Neijiang Normal University, Neijiang 641112, China; Beijing Computational Science Research Center, Beijing 100094, China;* orcid.org/0000-0002-9106-6333; Email: kwungyusung@gmail.com

Hui-Xiong Deng − *State Key Laboratory of Superlattices and Microstructures, Institute of Semiconductors, Chinese Academy of Sciences & Center of Materials Science and Optoelectronics Engineering, University of Chinese Academy*

of Sciences, Beijing 100083, China; orcid.org/0000-0003-2155-8727; Email: hxdeng@semi.ac.cn

Su-Huai Wei − *Beijing Computational Science Research Center, Beijing 100094, China;* orcid.org/0000-0003-1563-4738; Email: suhuaiwei@csrc.ac.cn

Author

Chen Qiu − *Beijing Computational Science Research Center, Beijing 100094, China;* orcid.org/0000-0003-4389-6671

Complete contact information is available at:
https://pubs.acs.org/10.1021/jacs.3c09808

Notes

The authors declare no competing financial interest.

REFERENCES

(1) Hall, R. N. Electron-Hole Recombination in Germanium. *Phys. Rev.* **1952**, *87*, 387−387.

(2) Shockley, W.; Read, W. T. Statistics of the recombinations of holes and electrons. *Phys. Rev.* **1952**, *87*, 835−842.

(3) Alkauskas, A.; Dreyer, C. E.; Lyons, J. L.; Van de Walle, C. G. Role of excited states in Shockley-Read-Hall recombination in wide-band-gap semiconductors. *Phys. Rev. B* **2016**, *93*, No. 201304.

(4) Kim, S.; Hood, S. N.; Walsh, A. Anharmonic lattice relaxation during nonradiative carrier capture. *Phys. Rev. B* **2019**, *100*, No. 041202.

(5) Berthe, M.; Stiufiuc, R.; Grandidier, B.; Deresmes, D.; Delerue, C.; Stievenard, D. Probing the carrier capture rate of a single quantum level. *Science* **2008**, *319*, 436−438.

(6) Henry, C. H.; Lang, D. V. Nonradiative capture and recombination by multiphonon emission in GaAs and GaP. *Phys. Rev. B* **1977**, *15*, 989−1016.

(7) Li, L.; Carter, E. A. Defect-mediated charge-carrier trapping and nonradiative recombination in WSe_2 monolayers. *J. Am. Chem. Soc.* **2019**, *141*, 10451−10461.

(8) Tong, C.-J.; Cai, X.; Zhu, A.-Y.; Liu, L.-M.; Prezhdo, O. V. How hole injection accelerates both ion migration and nonradiative recombination in metal halide perovskites. *J. Am. Chem. Soc.* **2022**, *144*, 6604−6612.

(9) Jiang, R.; Du, X.; Sun, W.; Han, Z.; Wu, Z. Enhancement of the blue photoluminescence intensity for the porous silicon with HfO_2 filling into microcavities. *Sci. Rep.* **2020**, *10*, 7171.

(10) Conley, J. F.; Lenahan, P. M.; Evans, H. L.; Lowry, R. K.; Morthorst, T. J. Observation and electronic characterization of two E' center charge traps in conventionally processed thermal SiO_2 on Si. *Appl. Phys. Lett.* **1994**, *65*, 2281−2283.

(11) Conley, J. F.; Lenahan, P. M.; Roitman, P. Evidence for a deep electron trap and charge compensation in separation by implanted oxygen oxides. *IEEE Trans. Nucl. Sci.* **1992**, *39*, 2114−2120.

(12) Bersuker, G.; Lee, B. H.; Huff, H. R.; Gavartin, J.; Shluger, A. *Mechanism of charge trapping reduction in scaled high-κ gete stacks*; Springer: Dordrecht, 2006.

(13) Zhao, C. Z.; Zahid, M. B.; Zhang, J. F.; Groeseneken, G.; Degraeve, R.; De Gendt, S. Properties and dynamic behavior of electron traps in HfO_2/SiO_2 stacks. *Microelectron. Eng.* **2005**, *80*, 366−369.

(14) Lu, W.-T.; Lin, P.-C.; Huang, T.-Y.; Chien, C.-H.; Yang, M.-J.; Huang, I.-J.; Lehnen, P. The characteristics of hole trapping in HfO_2/SiO_2 gate dielectrics with TiN gate electrode. *Appl. Phys. Lett.* **2004**, *85*, 3525−3527.

(15) Jiang, Z.; Li, X.; Zhou, X.; Wei, Y.; Wei, J.; Xu, G.; Long, S.; Luo, X. Experimental investigation on the instability for NiO/β-Ga_2O_3 heterojunction-gate FETs under negative bias stress. *J. Semicond.* **2023**, *44*, No. 072803.

(16) David, A.; Grundmann, M. J. Influence of polarization fields on carrier lifetime and recombination rates in InGaN based light-emitting diodes. *Appl. Phys. Lett.* **2010**, *97*, No. 033501.

(17) Warren, W. L.; Lenahan, P. M.; Brinker, C. J. Experimental evidence for two fundamentally different E′ precursors in amorphous silicon dioxide. *J. Non-Cryst. Solids* **1991**, *136*, 151−162.

(18) Pantelides, S. T.; Lu, Z. Y.; Nicklaw, C.; Bakos, T.; Rashkeev, S. N.; Fleetwood, D. M.; Schrimpf, R. D. The E′ center and oxygen vacancies in SiO_2. *J. Non-Cryst. Solids* **2008**, *354*, 217−223.

(19) Lu, Z. Y.; Nicklaw, C. J.; Fleetwood, D. M.; Schrimpf, R. D.; Pantelides, S. T. Structure, properties, and dynamics of oxygen vacancies in amorphous SiO_2. *Phys. Rev. Lett.* **2002**, *89*, No. 285505.

(20) Griscom, D. L.; Friebele, E. J. Fundamental radiation-induced defect centers in synthetic fused silicas atomic chlorine, delocalized E′ centers. *Phys. Rev. B* **1986**, *34*, 7524−7533.

(21) Buscarino, G.; Agnello, S.; Gelardi, F. M. Delocalized nature of the E'_δ center in amorphous sillicon dioxide. *Phys. Rev. Lett.* **2005**, *94*, No. 125501.

(22) Nicklaw, C. J.; Lu, Z. Y.; Fleetwood, D. M.; Schrimpf, R. D.; Pantelides, S. T. The structure, properties, and dynamics of oxygen vacancies in amorphous SiO_2. *IEEE Trans. Nucl. Sci.* **2002**, *49*, 2667−2673.

(23) Wang, L. Some recent advances in ab initio calculations of nonradiative decay rates of point defects in semiconductors. *J. Semicond.* **2019**, *40*, No. 091101.

(24) Jia, W.; Fu, J.; Cao, Z.; Wang, L.; Chi, X.; Gao, W.; Wang, L.-W. Fast plane wave density functional theory molecular dynamics calculations on multi-GPU machines. *J. Comput. Phys.* **2013**, *251*, 102−115.

(25) Jia, W.; Cao, Z.; Wang, L.; Fu, J.; Chi, X.; Gao, W.; Wang, L.-W. The analysis of a plane wave pseudopotential density functional theory code on a GPU machine. *Comput. Phys. Commun.* **2013**, *184*, 9−18.

(26) Schmidt, S. S.; Abou-Ras, D.; Sadewasser, S.; Yin, W.; Feng, C.; Yan, Y. Electrostatic potentials at $Cu(In,Ga)Se_2$ grain boundaries experiment. *Phys. Rev. Lett.* **2012**, *109*, No. 095506.

(27) Heyd, J.; Scuseria, G. E.; Ernzerhof, M. Hybrid functionals based on a screened Coulomb potential. *J. Chem. Phys.* **2003**, *118*, 8207−8215.

(28) Blöchl, P. E. First-principles calculations of defects in oxygen-deficient silica exposed to hydrogen. *Phys. Rev. B* **2000**, *62*, 6158−6179.

(29) Wei, S.-H. Overcoming the doping bottleneck in semiconductors. *Comput. Mater. Sci.* **2004**, *30*, 337−348.

(30) Pässler, R. Nonradiative multiphonon transitions described by static versus adiabatic coupling scheme in comparison with landau-zener's theory. *Czech J. Phys. B* **1982**, *32*, 846−883.

(31) Pässler, R. Description of nonradiative multiphonon transitions in the static coupling scheme. *Czech J. Phys. B* **1974**, *24*, 322−339.

(32) Shi, L.; Wang, L. W. Ab initio calculations of deep-level carrier nonradiative recombination rates in bulk semiconductors. *Phys. Rev. Lett.* **2012**, *109*, No. 245501.

(33) Shi, L.; Xu, K.; Wang, L.-W. Comparative study of ab initio nonradiative recombination rate calculations under different formalisms. *Phys. Rev. B* **2015**, *91*, No. 205315.

(34) Huang, K. Lattice relaxation and multiphonon transitions. *Contemp. Phys.* **1981**, *22*, 599−612.

(35) Chanana, R. K. Determination of hole effective mass in SiO_2 and SiC conduction band offset using Fowler−Nordheim tunneling characteristics across metal-oxide-semiconductor structures after applying oxide field corrections. *J. Appl. Phys.* **2011**, *109*, 104508.

(36) Brar, B.; Wilk, G. D.; Seabaugh, A. C. Direct extraction of the electron tunneling effective mass in ultrathin SiO_2. *Appl. Phys. Lett.* **1996**, *69*, 2728−2730.

(37) Boero, M.; Pasquarello, A.; Sarnthein, J.; Car, R. Structure and hyperfine parameters of E'_1 Centers in α-Quartz and in Vitreous SiO_2. *Phys. Rev. Lett.* **1997**, *78*, 887−890.

(38) Wimmer, Y.; El-Sayed, A. M.; Gos, W.; Grasser, T.; Shluger, A. L. Role of hydrogen in volatile behaviour of defects in SiO_2-based electronic devices. *Proc. R. Soc. A* **2016**, *472*, No. 20160009.

(39) Yang, J.-H.; Park, J.-S.; Kang, J.; Wei, S.-H. First-principles multiple-barrier diffusion theory: The case study of interstitial diffusion in CdTe. *Phys. Rev. B* **2015**, *91*, No. 075202.

(40) Guo, D.; Qiu, C.; Yang, K.; Deng, H.-X. Nonradiative carrier recombination enhanced by vacancy defects in ionic II-VI semiconductors. *Phys. Rev. Appl.* **2021**, *15*, No. 064025.

(41) Qiu, C.; Cao, R.; Wang, F.; Deng, H.-X. Large lattice-relaxation-induced intrinsic shallow p-type characteristics in monolayer black phosphorus and black arsenic. *Appl. Phys. Lett.* **2021**, *118*, No. 083102.